Asian Journal of Civil Engineering (2023) 24:969–988
https://doi.org/10.1007/s42107-022-00546-5

RESEARCH

Evaluation of the seismic performance of structures equipped with novel multi-level TADAS dampers

Arash Akbari Hamed[1] · **Seyedeh Fatemeh Mortazavi**[1] · **Mahsa Saeidzadeh**[1]

Received: 20 November 2022 / Accepted: 28 November 2022 / Published online: 7 December 2022

Abstract

Most dampers are designed for major earthquakes, while small earthquakes are likely to occur during the useful life cycle of buildings, and these smaller earthquakes may also damage structural and non-structural components; multi-level dampers are designed with a mechanism that works partly in minor earthquakes and partly in major earthquakes. Therefore, using these dampers prevents damage to structural and non-structural components at different levels of earthquakes. This study introduces the multi-level shear-bending TADAS damper and examines three types of multi-level TADAS dampers including: (1) a TADAS made by different steel grade materials, (2) a TADAS combined with friction pads and (3) a TADAS with different pin hole sizes. Moreover, further research is performed to evaluate the seismic performance of the multi-level TADAS damper in a 10-story building model using the incremental dynamic analysis (IDA). According to the obtained results, the considered models showed the expected seismic performance at two earthquake hazard levels which in turn indicates the usefulness of multi-level TADAS dampers in seismic energy dissipation. Examination of IDA curves shows that the effective yield and the collapse points of structures equipped with multi-level TADAS dampers occur in about 53.1% and 143.5% higher earthquake intensities compared to the structures without dampers, respectively. Moreover, due to the enhanced seismic performance of these systems, lightweight structures can be designed which is in line with the goals of sustainable development which is another advantage of this system.

Keywords Metallic yielding damper · Friction damper · Multi-level damper · TADAS damper · Incremental dynamic analysis

Introduction

Earthquakes are one of the natural disasters that sometimes cause great loss of life and cost in urban societies. Because it is practically impossible to evacuate the city even if earthquakes are predicted, seismic-resistant buildings must be built. Due to the uncertainty in determining the large seismic forces acting on the structures, it will be uneconomical to design the structures so that they remain in the elastic range during an earthquake; therefore, the structures are designed to behave inelastically during the design earthquake to dissipate a large amount of the input seismic energy. In this regard, predetermined fuse-like elements are considered in structural systems to experience major deformations during an earthquake to dissipate the seismic energy and keep the main members in the elastic behavior range without any damage (Hamed & Basim, 2020; Nobari & Hamed, 2017; Saeidzadeh et al., 2022a, 2022b). The dampers are one of the fuse-like elements which can be used in four types including: active control, semi-active control, hybrid control, and passive control. The mechanism of active control is mainly used for viscous (Ribakov, 2001) and tuned mass dampers (Fahimi Farzam & Kaveh, 2020; Kaveh et al., 2015, 2020a, 2020b). However, passive structural control systems are used frequently due to their no need for external energy such as electricity and stable hysteretic behavior and the low cost of production and the simplicity of design compared to the other types of structural control systems. Passive dampers

✉ Arash Akbari Hamed
akbarihamed.a@sut.ac.ir

Seyedeh Fatemeh Mortazavi
SF_mortazavi@sut.ac.ir

Mahsa Saeidzadeh
mahsa.saeidzadeh@yahoo.com

[1] Faculty of Civil Engineering, Sahand University of Technology, Tabriz, Iran

are also classified into two groups: velocity-dependent dampers and displacement-dependent dampers. Velocity-dependent dampers reduce structural vibrations only by increasing damping, while displacement-dependent dampers, such as metallic yielding dampers reduce structural seismic responses by adding stiffness and damping to the structures. In 1972, Kelly et al. proposed the metallic yielding dampers as an effective passive control system and this novel idea was followed by Skinner et al. to develop several types of hysteretic dampers which behaved inelastically in various combinations of torsional, flexural and shear deformations (Kelly et al., 1972; Skinner et al., 1974). Metallic yielding dampers are divided into two types including: flexural yielding dampers and shear yielding dampers. The most common types of flexural yielding dampers are Added Damping and Stiffness (ADAS) dampers and Triangular ADAS (TADAS) dampers. These dampers consist of several parallel steel plates placed between two rigid plates and dissipate the seismic energy based on the flexural yielding of parallel plates. In 1993, Tsai et al. proposed a way to design structures equipped with TADAS dampers and based on the obtained experimental results, it was concluded that properly designed TADAS dampers did not show any strength and stiffness degradation (Tsai et al., 1993). In 2008, Alehashem et al. examined the behavior and performance of steel structures equipped with ADAS dampers and compared the behavior of this system with that of conventional steel braced frames and the results showed that the main members of the considered structures were kept safe while the inelastic behavior was concentrated in the installed dampers (Alehashem, et al., 2008). In 2010, Abdollahzadeh and Bayat studied the behavior of structures equipped with ADAS dampers under far-field records and presented some codes and solutions to optimize their seismic performance (Abdollahzadeh & Bayat, 2010). Rezaei et al. assessed the seismic performance of dissipative column dampers consisting of several adjacent columns joined together with X-shaped metallic yielding dampers under far-field and near-field records (Rezaei et al., 2020). Moreover, shear yielding dampers have several spans that are subjected to shear deformations and dissipate the input seismic energy through the plastic shear yielding of the infill panels. One of the various types of shear yielding dampers include shear panel dampers, which usually have an I-shaped configuration, in which the web plate is used to dissipate energy under shear deformation, and the flanges on both sides of the web plate are used to provide the required stiffness and constraint at the ends of the web plate. As a result, the web plate may be uniformly yielded, while the flanges remain quite elastic. Moreover, the analytical and experimental studies on the investigation of the seismic performance of shear panels alone and in combination with braces indicated the acceptable energy absorption capacity of this type of damper (Akbari Hamed & Mofid, 2015a, 2015b, 2017; Hamed et al., 2021).

In recent years, multi-level dampers have been introduced in which the input seismic energy is dissipated in both small and large earthquakes. The installation of these dampers prevents damage to the main members of the structures at different earthquake levels and reduces the required cost and time for replacing the yielded common one-level dampers. The novel idea of multi-level performance can be used in TADAS dampers that have a simple manufacturing method with better performance compared to normal TADAS dampers (Hosseini Hashemi & Moaddab, 2017). In the following, some of the approaches making a multi-level TADAS damper are presented. The first solution is to change the materials used in the parallel triangular plates such that during an earthquake and hence the horizontal relative movement of the top and bottom of the damper, all the triangular plates are deformed; but because their yield strength is different, these plates do not yield at the same time. Therefore, the damper behaves inelastically at different earthquake levels and dissipates energy (Mosayebi et al., 2016). Another method is to assign pin holes with different sizes in the place where the triangular plates are connected to the body of the damper, in which case, after a certain displacement, the triangular plates with larger holes behave inelastically in main earthquakes. Combining different damping mechanisms is another way to make a multi-level TADAS damper in which the friction pads can be used as the auxiliary damping system for the dissipation of seismic energy of minor earthquakes. It should be noted that due to the stable behavior of friction dampers, they are more suitable for moderate earthquakes that are more likely to occur. In 2011, Hashemi and Dareini studied the seismic behavior of structures at different earthquake levels using modified-TADAS dampers in which a series of plates start working at minor earthquakes whereas the second set of plates is still elastic and they would dissipate the seismic energy at major earthquakes. The results showed that the modified-TADAS dampers enhanced the performance of the considered structures (Hashemi and Dareini, 2011). In 2014, Li et al. tested the metallic yielding-friction damper in which the main idea was that the input energy of small earthquakes would be dissipated by the friction component while metallic yielding damper would work in large earthquakes (Li et al., 2014). In 2017, Hosseini Hashemi and Moaddab tested a hybrid damper with a dual function design as an alternative to standard metallic yielding and friction dampers. They studied a multi-level TADAS damper with dual function (D-TADAS) and another combined device made of friction damper and TADAS damper (Hosseini Hashemi & Moaddab, 2017). Moreover, Mosayebi et al. researched modifying the performance of TADAS dampers under different

earthquake levels by changing the materials of triangular plates (Mosaybi et al., 2016). Li et al. introduced a shear-bending metallic yielding damper which consisted of a shear panel and a series of K-shaped plates to prevent the out-plane buckling of the shear panel. They concluded that the interactively working of the shear and bending components enhance the individual performance of these components (Li et al., 2019).

Due to the importance of providing multi-level dampers to enhance the seismic performance of structures at different seismic hazard levels, this research introduces the multi-level shear-bending TADAS damper and examines three types of multi-level TADAS dampers including (1) a TADAS made by different steel grade materials, (2) a TADAS combined with friction pads and (3) a TADAS with different pin hole sizes. To this aim, the considered finite element modeling procedure was validated based on the existing results of two experimental specimens. Then, five multi-level damper models with different energy dissipation mechanisms were examined using ABAQUS software under cyclic loadings. Finally, the best damper in terms of stiffness, energy dissipation, and ductility was selected. Then, a two-dimensional 10-story steel frame equipped with the selected multi-level damper was analyzed by the IDA method to investigate its seismic performance.

Description of the performance of multi-level TADAS dampers

Given a bi-linear behavior for the metallic yielding main and auxiliary fuses, Fig. 1 shows a schematic force–displacement diagram of a multi-level TADAS damper.

Figure 1a shows the bi-linear behavior of the auxiliary fuse in which K_a and αK_a are the elastic stiffness and post-yielding stiffness, respectively. The auxiliary fuse yields at a point with δ_{ya} and f_{ya} coordinates which show the corresponding values of the effective yielding displacement and the effective yielding force, respectively. Equations 1 and 2 describe the force (f)–displacement (u) relationship of the multi-level TADAS damper for minor earthquakes.

$$u \le \delta_{ya} \Rightarrow f = K_a u, \tag{1}$$

$$\delta_{ya} < u \le \delta_m \Rightarrow f = \alpha K_a\left(u - \delta_{ya}\right) + f_{ya}, \tag{2}$$

where δ_m is the displacement value after which the main fuse starts working at major earthquakes. Figure 1b depicts the bi-linear behavior of the main fuse in which K_m and $\alpha' K_m$ are the elastic stiffness and post-yielding stiffness, respectively. The main fuse yields at a point with δ_{ym} and f_{ym} coordinates which show the corresponding values of the effective yielding displacement and the effective yielding force, respectively. Moreover, Fig. 1c shows the total response of the multi-level TADAS damper in which the force–displacement relationships of the damper after the contribution of the main fuse, can be achieved using Eqs. 3 and 4.

$$\delta_m < u \le \delta_{ym} \Rightarrow f = \alpha K_a\left(u - \delta_{ya}\right) + f_{ya} + K_m\left(u - \delta_m\right), \tag{3}$$

$$u \ge \delta_{ym} \Rightarrow f = \alpha K_a\left(u - \delta_{ya}\right) + f_{ya} + f_{ym} + \alpha' K_m\left(u - \delta_{ym}\right). \tag{4}$$

If a friction mechanism is used as the auxiliary fuse, the resulting force–displacement diagram of the combined multi-level damper is changed as shown in Fig. 2.

Equation 5 describes the behavior of the auxiliary fuse in which f_{fa} is the slip force which is calculated by multiplying the coefficient of friction by the considered normal force (Fig. 2a).

$$0 < u \le \delta_m \Rightarrow f = f_{fa}. \tag{5}$$

Considering a bi-linear behavior for the main fuse which starts working at δ_m (Fig. 2b), the total response of the multi-level combined TADAS damper is obtained as shown in Fig. 2c and the describing force–displacement relationships of this damper can be achieved using Eqs. 6 and 7.

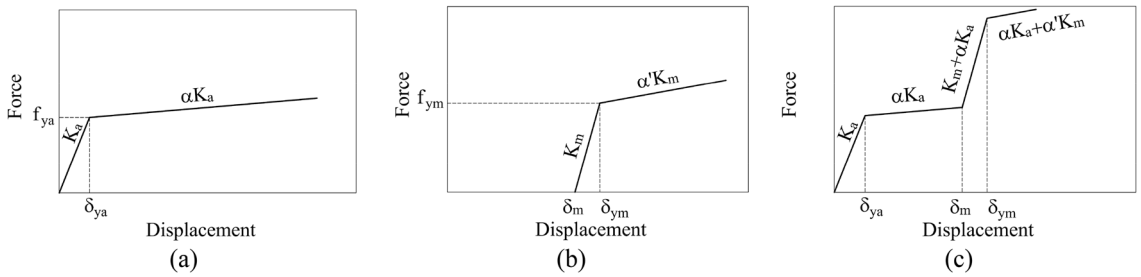

Fig. 1 Schematic force–displacement diagram of a multi-level TADAS damper: **a** the auxiliary fuse, **b** the main fuse and **c** Total response of the multi-level damper

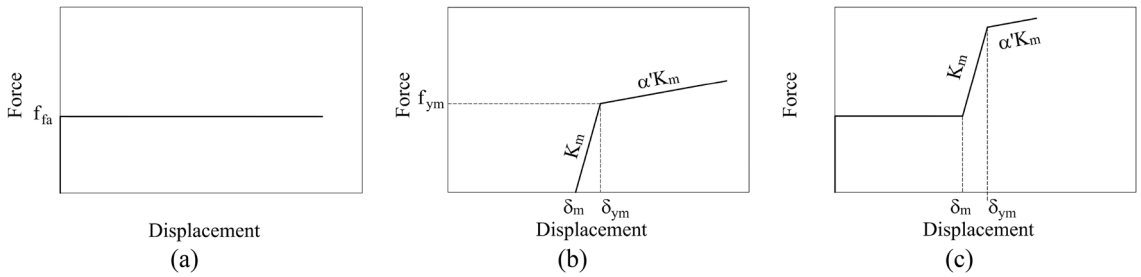

Fig. 2 Schematic force–displacement diagram of a multi-level combined TADAS with friction pad damper: **a** the auxiliary fuse, **b** the main fuse and **c** total response of the multi-level damper

$$\delta_m < u \le \delta_{ym} \Rightarrow f = f_{fa} + K_m\left(u - \delta_m\right), \tag{6}$$

$$u \ge \delta_{ym} \Rightarrow f = f_{fa} + f_{ym} + \alpha' K_m\left(u - \delta_{ym}\right). \tag{7}$$

Verification of the finite element modeling method

To verify the considered finite element modeling method, the multi-level dampers of D-TADAS and FD-TADAS were modeled using ABAQUS and the obtained analytical results were compared with the experimental results which were obtained by Hosseini Hashemi and Moaddab (2017).

The D-TADAS-2PL damper

The D-TADAS-2PL was a metallic yielding TADAS damper which consisted of two triangular plates. The assigned pin hole at the end of the auxiliary plate was a slotted hole which had a width equal to the diameter of the pin (i.e. 20 mm) while the assigned pin hole to the main plate had a width of 50 mm which was 15 mm larger than the pin diameter from each side. Both plates had a height of 180 mm and their width was changed linearly from 80 mm at the top of plates to 20 mm at the bottom of plates. Moreover, the thickness of the main and auxiliary plates was 20 and 22 mm, respectively. The pin has a length of 40 mm and a PL140 × 120 × 20 mm was used as the perforated plate. Figure 3 shows the geometrical properties of components of the D-TADAS-2PL damper.

The material properties of steel grade A36 (Table 1) were assigned to both plates using the combined hardening option (i.e. parameters and cyclic hardening) in ABAQUS. where E = elastic modulus, ν = Poisson's ratio, σ_y = yield strength, Q_∞ & b = isotropic hardening parameters and C_1 and γ_1 = kinematic hardening parameters. As depicted in Fig. 4, the considered cyclic quasi-static loading protocol was applied to the top plate of the model as the displacement boundary condition.

By defining a combination of the tangential behavior of friction type and the normal behavior of hard contact type, the surface-to-surface contact (standard) method was used to create the interaction between the pin and the wall of the holes. It should be mentioned that the tangential friction behavior was defined with penalty formulation and a friction coefficient of 0.3 was assigned. The interaction between other parts of the model was defined using the Tie contact. The assigned average mesh size for the model was 7 mm

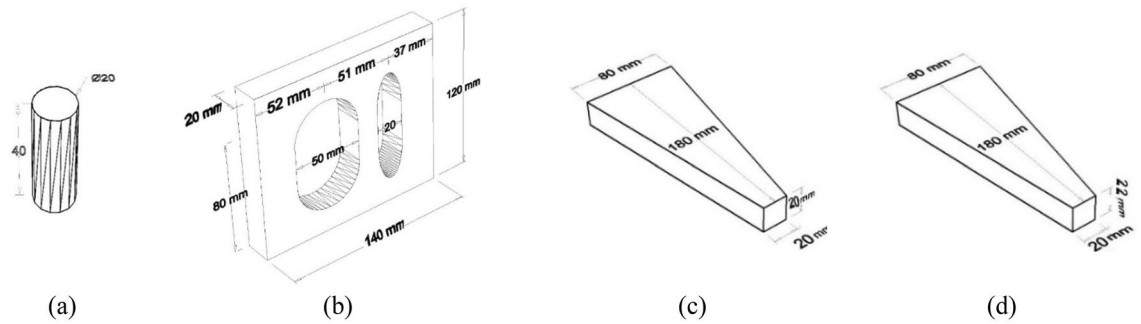

Fig. 3 The geometrical properties of components of the D-TADAS-2PL model: **a** the pin, **b** the perforated plate, **c** the main triangular plate, **d** the auxiliary triangular plate (all dimensions are in mm)

Table 1 The considered material properties of the steel grade A36 for the D-TADAS-2PL model

E [MPa]	ν	σ_y [MPa]	Isotropic hardening parameters (Payne, 2000)		Kinematic hardening parameters (Payne, 2000)	
			Q_∞ [MPa]	b	C_1 [MPa]	γ_1
2.01×105	0.3	261	137.89	10	3447	50

and the C3D8R elements were used. As shown in Fig. 5, it is observed that comparing the obtained hysteretic curves and the deformation status of the finite element model at the end of loading (i.e. at a displacement of 75 mm) are perfectly consistent with the ones of the experimental specimen which was tested by Hosseini Hashemi and Moaddab (2017).

The FD-TADAS-3PL damper

The FD-TADAS-3PL damper was a combination of a metallic yielding TADAS damper as the main damper and a friction pad as the auxiliary damper (Hosseini Hashemi & Moaddab, 2017). Figure 6 shows the geometrical properties of different parts of the FD-TADAS-3PL model in which the upper part (i.e. main damper) consists of triangular plates, perforated plates and pins, and the lower part (i.e. auxiliary damper) consists of the friction pad and the bottom plate. It should be noted that 4 steel rods at a distance of 15 mm from the ends of the upper part were placed in the corners of the bottom plate such that when the major earthquakes occur, the upper part meets the steel rods as the end barriers and the main damper starts working. The material properties of steel grade A36 (Table 1) were assigned to this model using the combined hardening option (i.e. Parameters and Cyclic hardening) in ABAQUS and the friction pad was considered as a brass plate (i.e. UNS-260) which has $E = 1.1 \times 10^5$ MPa and $\nu = 0.38$.

By defining a combination of the tangential behavior of friction type and the normal behavior of hard contact type, the surface-to-surface contact (standard) method was defined to create the interaction between the different moving parts of the model. It should be mentioned that the tangential friction behavior was defined with penalty formulation and a friction coefficient of 0.3 was assigned. The interaction between other parts of the model, which had no relative movement to each other, was defined using the Tie contact. The assigned mesh size for different parts of the model was changed while its average value was 6 mm and the C3D8R elements were used. Moreover, due to the simplicity of the modeling procedure, only one layer of friction pad was modeled and an equivalent normal load of 22 kN was applied to the model to have the same amount of friction force same as the tested experimental specimen. The considered cyclic quasi-static loading protocol was applied to the top plate of the model (Fig. 4). As shown in Fig. 7, it is observed that comparing the obtained hysteretic curves and the deformation status of the finite element model at the end of loading (i.e. at a displacement of 75 mm) are perfectly consistent with the ones of the experimental specimen which was tested by Hosseini Hashemi and Moaddab (2017). It is noteworthy that the considered loading protocol in the reference of (Hosseini Hashemi & Moaddab, 2017) was not available until the end of the performed test (i.e. to the displacement of 120 mm), therefore, the numerical analysis was continued up to the displacement of 75 mm.

Due to the completely restrained horizontal edges of the considered finite element models, there is a concern that the rotation of the TADAS dampers as a result of the lateral displacement of the frame can have an adverse effect on their structural performance. In this regard, it should be mentioned that Hosseini Hashemi and Moaddab (2017) performed the universal test of the D-TADAS-4PL specimen and the cyclic test of a frame equipped with a D-TADAS-4PL damper. It is noteworthy that all the geometrical and material properties of the considered D-TADAS-4PL dampers in these two tests were the same except for the height of the triangular plates which was 180 mm in the universal test and 170 mm in the frame test. Regarding the obtained results in the experimental study performed by Hosseini Hashemi and Moaddab (2017), it was seen that the shape of the obtained hysteretic curves along with the multi-level performance of the D-TADAS-4PL dampers for both the performed tests were similar. The only difference was the amount of strength which was mainly due to the considered different triangular plates' heights. Therefore, it is concluded that the amount of rotation of the main body of the TADAS dampers mounted on the chevron braces will be negligible

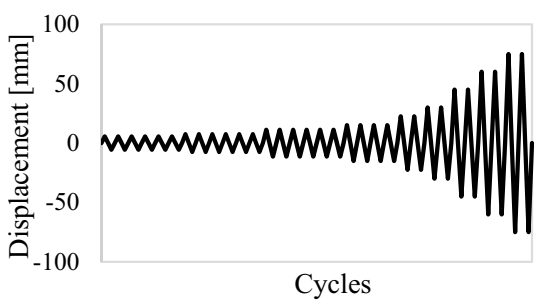

Fig. 4 The applied cyclic quasi-static loading protocol

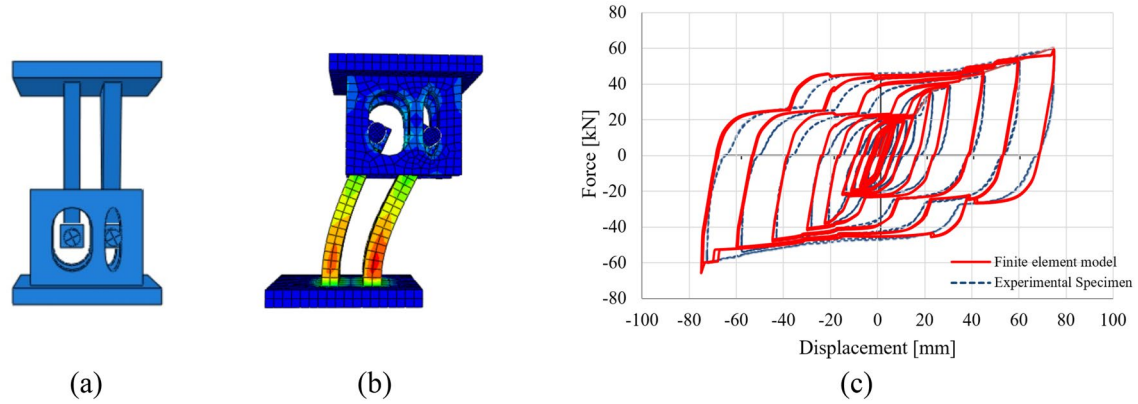

Fig. 5 **a** The D-TADAS-2PL model, **b** the deformation status at a displacement of 75 mm, **c** comparison of the obtained experimental and numerical hysteretic curves

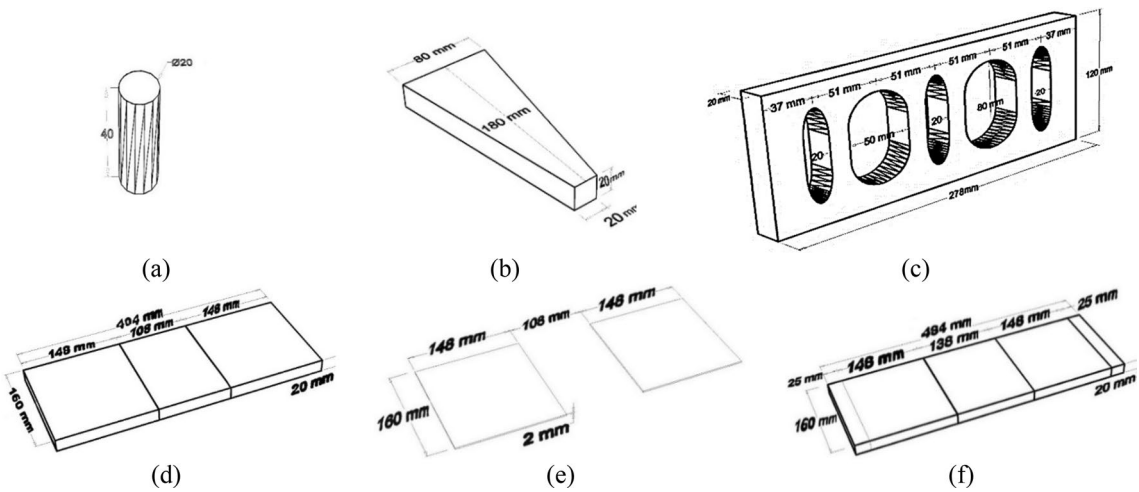

Fig. 6 The geometrical properties of components of the FD-TADAS-3PL model: **a** the pin, **b** the triangular plate, **c** the perforated plate, **d** the plate between the perforated plate and the friction pad, **e** the friction pad, **f** the bottom plate (all dimensions are in mm)

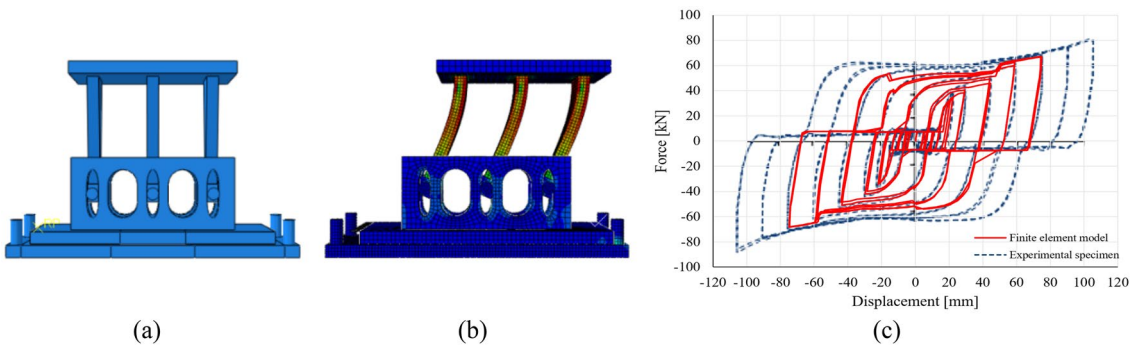

Fig. 7 **a** The FD-TADAS-3PL model, **b** the deformation status at a displacement of 75 mm, **c** comparison of the obtained hysteretic curves

and it will not affect the performance of the installed damper. Moreover, it should be mentioned that regarding the specifications of existing structural steel building codes, all the geometrical imperfections in the preparation of structural members should be within the range of permissible tolerances. Based on the numerical and experimental studies,

observing the allowed tolerances and minimized manufacturing errors (i.e. geometrical imperfections) will not significantly affect the performance of structural members including dampers. Therefore, it is forbidden to exceed the amount of geometrical imperfections from the permitted values of the existing structural steel provisions, and in such a situation, the structural members must be rebuilt. Moreover, the existence of initial imperfections such as the mild distortion or deformation of a steel plate may have significant adverse effects on the performance of a structural member made by very thin plates (e.g. ≅ 0.3 to 5 mm); but, as the thickness of triangular plates in the considered multi-level TADAS dampers of this study were equal to 22 mm and 20 mm, then it seems that the amount of any initial imperfections and their possible negative consequences on the structural performance may be negligible. However, investigating the issue of negative consequences of possible geometrical imperfections on the performance of structural members and ensuring that the negative effects of permitted tolerance values are negligible deserve to be evaluated in future studies.

Investigation of the performance of different types of multi-level TADAS dampers

In this section, the performance of the following five multi-level TADAS dampers under the considered cyclic quasi-static loading protocol (Fig. 4) was examined.

1. The D-TADAS-3PL model with 2 main fuse plates and 1 auxiliary fuse plate.
2. The D-TADAS-5PL model with 3 main fuse plates and 2 auxiliary fuse plates.
3. The FD-TADAS-5PL model in which 5 TADAS plates and 1 friction pad act as the main fuse and the auxiliary fuse, respectively.
4. The SP-TADAS-2PL model in which 2 TADAS plates and 1 shear panel act as the main fuse and the auxiliary fuse, respectively.
5. The TADAS-DIFFMAT model in which two types of materials with different yield strengths act as the main fuse and the auxiliary fuse.

It is noteworthy that the dampers of D-TADAS-2PL and FD-TADAS-3PL consist of metallic yielding and friction damping mechanisms, both of which were validated based on the research performed by Hosseini Hashemi and Moaddab (2017). Then, the SP-TADAS-2PL and TADAS-DIFFMAT models which are categorized as metallic yielding dampers, were modeled with the same verified modeling method. It should be noted that the structural interstory drift ratio should not exceed 0.005 in small or serviceability earthquakes (Standard-2800, 2014; Garevski and Ansal, 2010), and as the typical story height is 3 m, hence, a displacement value of 15 mm was considered as the design criterion of the studied dampers. In other words, the considered dampers were designed in such a way that there was a 15 mm displacement gap between the starting point of the main and auxiliary fuses. It is noteworthy that in this study, a numerical study was performed on different possible ways to have multi-level TADAS dampers and a new one was proposed. As the considered finite element procedure was validated based on the experimental study carried out by Hosseini Hashemi and Moaddab (2017), therefore the same geometrical dimensions with a few changes were considered in all various models. Moreover, to compare the performance of different dampers, their geometrical and material properties must be considered the same. For example, the geometrical dimensions of the shear panel in the SP-TADAS-2PL model and the yield strength of the main plates of the TADAS-DIFFMAT model were determined by the trial-and-error approach to meet the only design criterion which was the drift limit considered for serviceability earthquake. In other words, the dimensions of triangular plates in the considered different models were kept constant and the other dimensions were determined using a displacement-based design approach.

The D-TADAS-3PL and D-TADAS-5PL models

The D-TADAS-3PL and D-TADAS-5PL models were modeled using the same validated method in Sect. 3. The assigned material properties of these models and the applied loading protocol were similar to Table 1 and Fig. 4, respectively. Table 2 shows the specifications of D-TADAS-5PL and D-TADAS-3PL models.

Figure 8 depicts the finite element models of D-TADAS-3PL and D-TADAS-5PL dampers and the corresponding obtained hysteretic and envelope curves. As shown in Fig. 8, the obtained envelope curves were linearized based on the recommended energy method of FEMA-356 (2000a). It should be noted that to recognize the multi-level action of the considered dampers, the envelope curve of each performance level was linearized to a bi-linear curve; therefore, it is seen that the linearized curves are a combination of

Table 2 Specifications of D-TADAS-5PL and D-TADAS-3PL models

Model	No. of main plates	Main plates' thickness [mm]	No. of auxiliary plates	Auxiliary plates' thickness [mm]	Gap [mm]
D-TADAS-5PL	3	20	2	22	15
D-TADAS-3PL	2	20	1	22	15

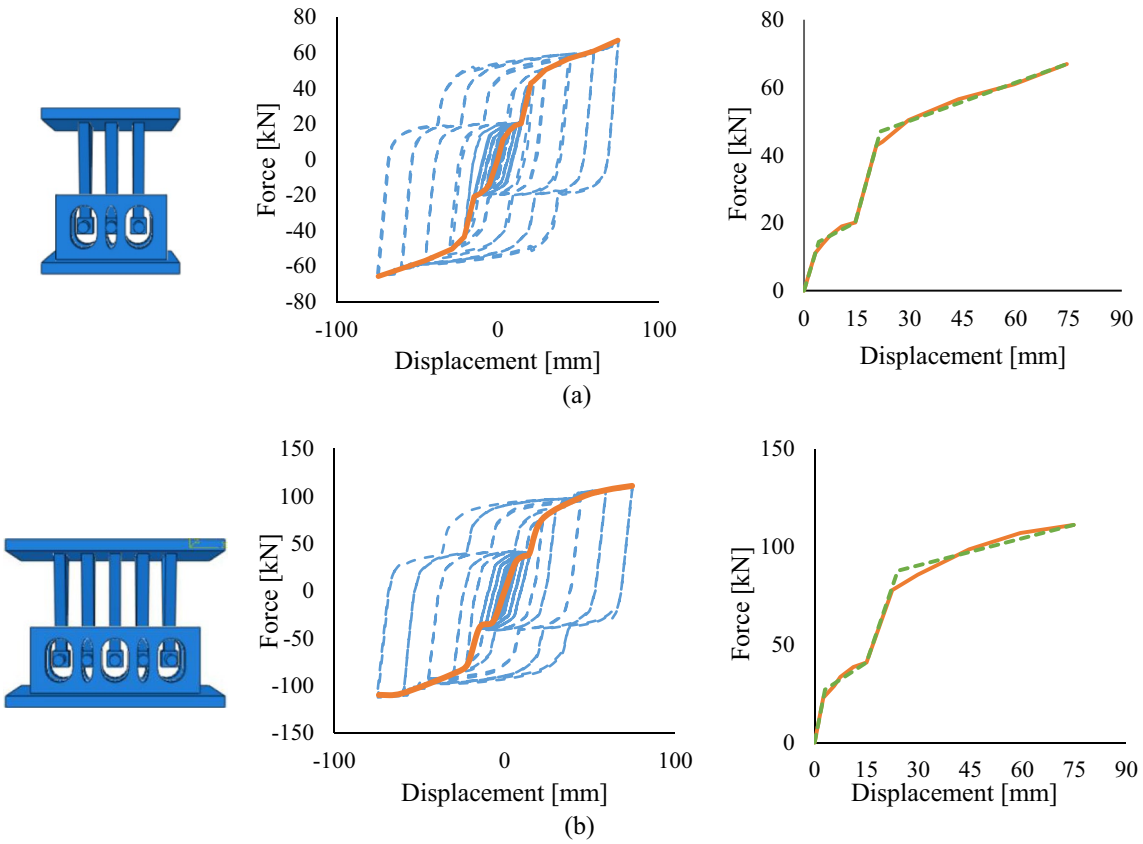

Fig. 8 The finite element models and obtained hysteretic, envelope (orange solid line) and linearized (green dashed line) curves: **a** D-TADAS-3PL, **b** D-TADAS-5PL

two bi-linear diagrams. Regarding the linearized curves, it is seen that the considered design criterion was fully observed and the main fuses started working at a displacement of 15 mm.

As shown in Fig. 9, it is observed that at a displacement value of 15 mm, only the auxiliary fuses yielded (i.e. AC yield value of 1 and the Von Mises stress value of more than 261 MPa) whereas at the end of loading (i.e. at the displacement of 75 mm), all of the plates yielded.

The FD-TADAS-5PL model

The FD-TADAS-5PL model consisted of five triangular plates as the main fuse and the friction pad as the auxiliary fuse and it was modeled using the same validated method

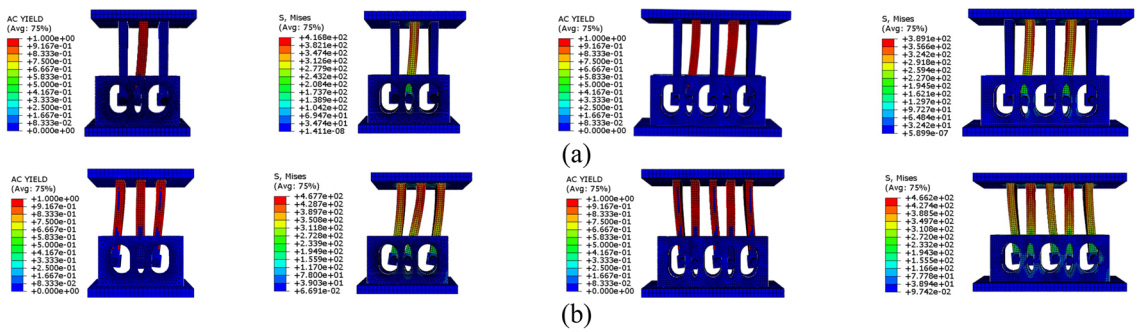

Fig. 9 The yielded regions and Von Mises stress distribution of D-TADAS-3PL and D-TADAS-5PL models at a displacement of: **a** 15 mm, **b** 75 mm

in Sect. 3. Moreover, the displacement value of 15 mm was considered as the design criterion for starting point of the main fuse. The assigned steel material properties of this model were similar to Table 1 and the friction pad was considered as a brass plate (i.e. UNS-260) which has $E = 1.1 \times 10^5$ MPa and $\nu = 0.38$. Figure 10 depicts the finite element model of FD-TADAS-5PL damper and corresponding hysteretic and envelope curves which were obtained by application of the cyclic quasi-static loading protocol shown in Fig. 4. Regarding the linearized curves, it is seen that the considered design criterion was fully observed and the main fuses started working at a displacement of 15 mm.

As shown in the Von Mises stress contour of Fig. 11a, it is observed that before starting to work of the main fuse (i.e. at displacements less than 15 mm), the stress developed only in the plates around the friction pad without any yielding in the model. However, the triangular plates of the main fuse started to yield at a displacement of 22 mm and the final yielding status of the model at the displacement of 75 mm is shown in Fig. 11b which shows the AC yield status along with the Von-Mises stress distribution of the model. Regarding Fig. 11b, it is seen that only the triangular plates, which experienced stresses more than 261 MPa, were yielded and the remaining parts of the FD-TADAS-5PL damper remained elastic.

The SP-TADAS-2PL model

This study introduces the multi-level SP-TADAS-2PL model in which a shear panel was used as the auxiliary fuse and two triangular plates were considered as the main fuse. To develop a complete tension-field action in the shear panel, two additional flange-like elements perpendicular to the shear panel plane were considered to form an I-shaped cross-section. Moreover, to provide a multi-level performance of this damper, the diameter of the assigned holes at the perforated plate, to which the triangular plates are connected, was considered 30 mm larger than the pin diameter (i.e. 15 mm from each side of the center of the pin). The geometrical properties of the SP-TADAS-2PL model are shown in Fig. 12 and the material properties were assigned to this model according to Table 1.

Figure 13 depicts the finite element model of SP-TADAS-2PL and corresponding obtained hysteretic and envelope curves which were obtained by application of the cyclic quasi-static loading protocol shown in Fig. 4. Regarding Fig. 13, it is observed that due to buckling of the shear panel and following the development of tension-field action (i.e. post-buckling behavior), pinching of the hysteretic curve and strength and stiffness deterioration occurred. However, regarding the linearized curves, it is seen that the considered design criterion was fully observed and the main fuses started working at a displacement of 15 mm.

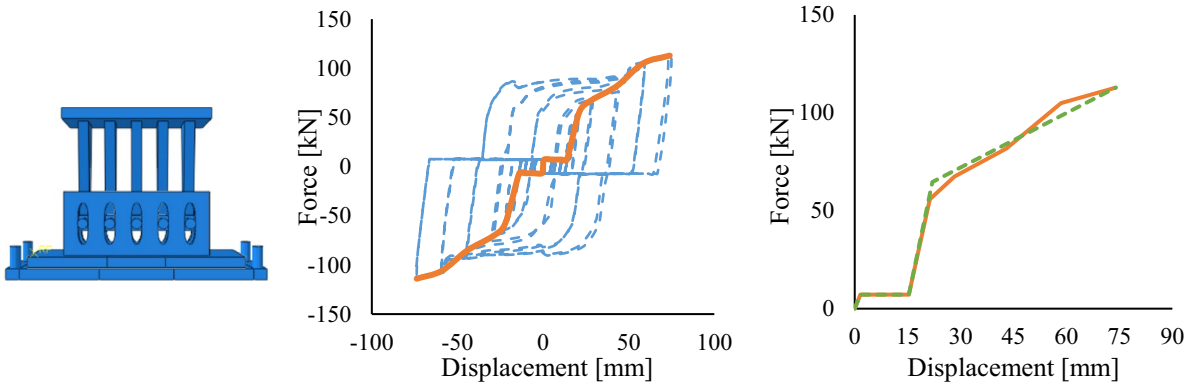

Fig. 10 The finite element FD-TADAS-5PL model and obtained hysteretic, envelope (orange solid line) and linearized (green dashed line) curves

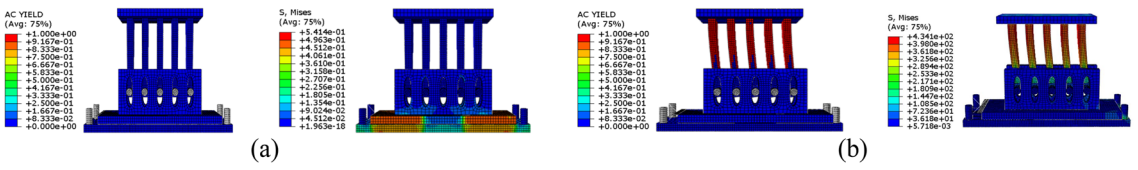

Fig. 11 The yielding status and Von Mises stress distribution of FD-TADAS-5PL model at a displacement of **a** less than 15 mm, **b** 75 mm

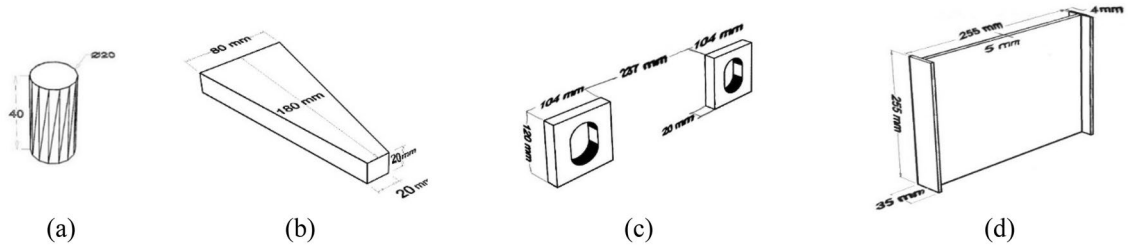

Fig. 12 The geometrical properties of the SP-TADAS-2PL model: **a** the pin, **b** the triangular plate, **c** the perforated plate, **d** the shear panel (all dimensions are in mm)

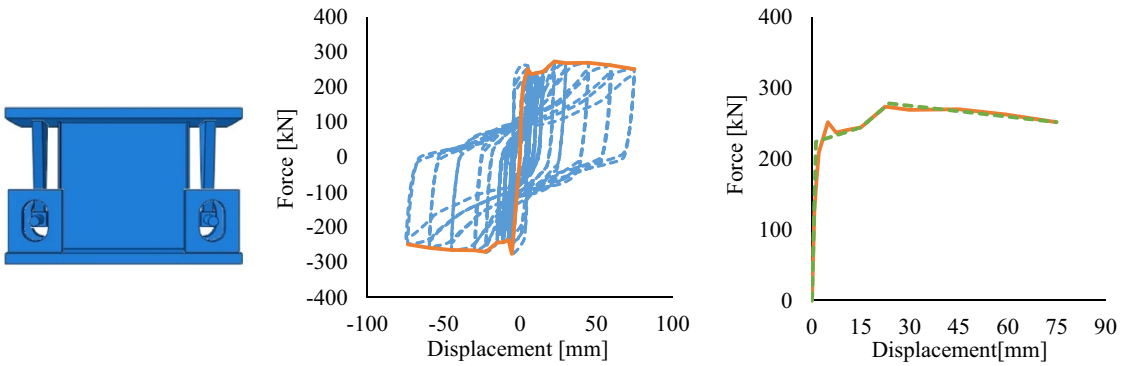

Fig. 13 The finite element SP-TADAS-2PL model and obtained hysteretic, envelope (orange solid line) and linearized (green dashed line) curves

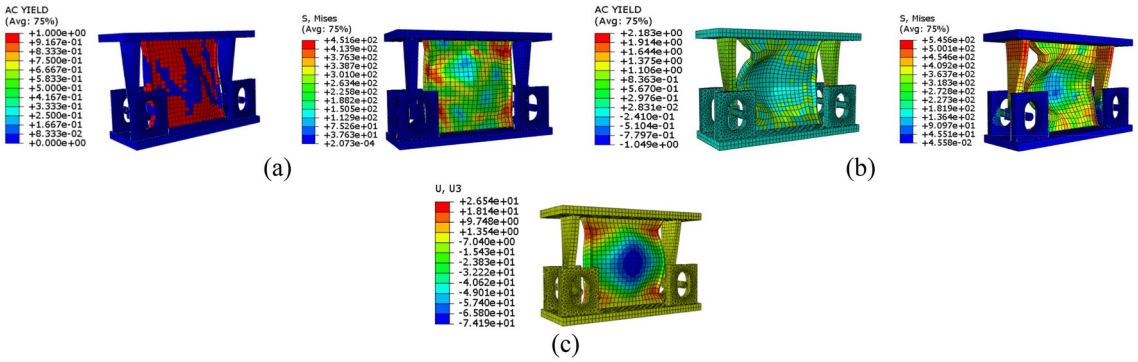

Fig. 14 The status of SP-TADAS-2PL model: a) the yielding status and Von Mises stress distribution at a displacement of less than 15 mm, b) the yielding status and Von Mises stress distribution at the displacement of 75 mm, c) the out-of-plane deformation of the model at the end of analysis

As shown in Fig. 14a, it is observed that before starting to work of the main fuse (i.e. at displacements less than 15 mm), only the shear panel yielded. However, the triangular plates of the main fuse started to yield after the design criterion of 15 mm and the final yielding status of the model along with the amount of out-of-plane deformation of the shear panel at the displacement of 75 mm are shown in Fig. 14b and c. It should be mentioned that the yield strength of steel material in this model was 261 MPa and considering the depicted Von Mises stress distribution contours, the yielded regions are determined.

Table 3 Specifications of the TADAS-DIFFMAT model

Model	No. of plates	Height [mm]	Thickness [mm]	Top width [mm]	Bottom width [mm]
The auxiliary damper	2	180	22	80	20
The main damper	3	180	20	80	20

The TADAS-DIFFMAT model

The TADAS-DIFFMAT model consisted of five triangular plates which were made of different steel grade materials (Table 3) and it was modeled using the same validated method in Sect. 3. In this multi-level TADAS damper, the yield strength of the main fuse plates was higher than the auxiliary fuse plates in such a way that before reaching the displacement of 15 mm, only the auxiliary plates dissipated the input seismic energy and after meeting the design criterion of 15 mm, the main plates started working and yielded. The assigned steel material to the auxiliary plates and main plates had a yield strength of 261 MPa and 360 MPa, respectively.

Figure 15 depicts the finite element model of the TADAS-DIFFMAT damper and corresponding hysteretic and envelope curves which were obtained by the application of the cyclic quasi-static loading protocol shown in Fig. 4. Regarding the linearized curves, the multi-level performance of this damper is visible and it is concluded that the considered design criterion was fully observed and the main fuses started working at a displacement of 15 mm. In other words, at first, all of the triangular plates behaved elastically, and then the auxiliary plates yielded at a displacement of approximately 5 mm, and finally, after a displacement of 15 mm, the main plates also yielded.

As shown in Fig. 16a, it is observed that before starting to work of the main fuse (i.e. at displacements less than 15 mm), the auxiliary plates fully yielded and by approaching the design criterion of 15 mm, the outer fibers of main dampers yielded partially; but, after the displacement value of 15 mm, the main plates yielded completely and their contribution in dissipation of seismic energy was increased considerably (e.g. the Von-Mises stress values more than 261 MPa and 360 MPa for the auxiliary and main plates, respectively) (Fig. 16b).

The best multi-level TADAS damper

The purpose of this section is to select the best multi-level TADAS damper based on the obtained hysteretic curves and their performance parameters such as elastic stiffness,

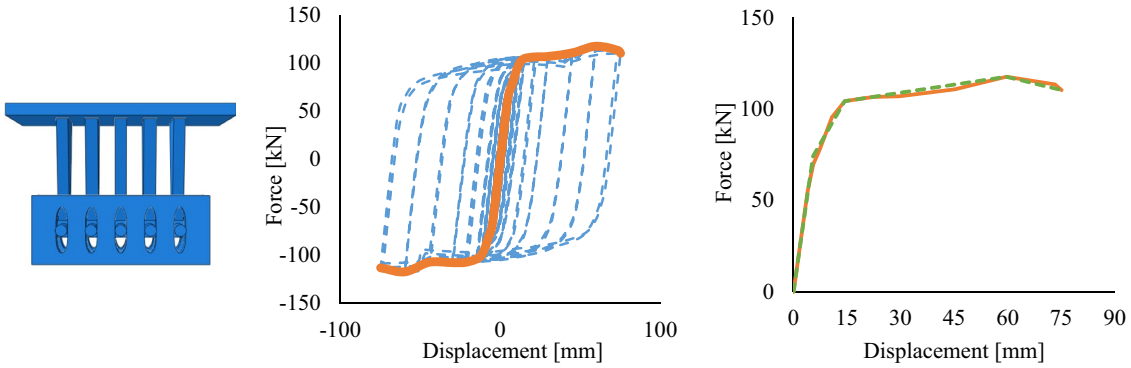

Fig. 15 The finite element TADAS-DIFFMAT model and obtained hysteretic, envelope (orange solid line) and linearized (green dashed line) curves

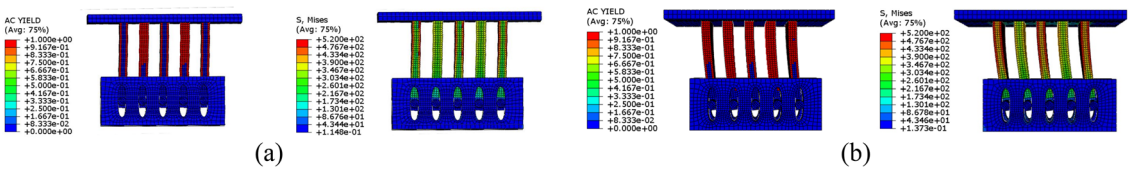

Fig. 16 The yielding status and Von Mises stress distribution of TADAS-DIFFMAT model at a displacement of **a** less than 15 mm, **b** more than 15 mm

Table 4 The calculated values of the mentioned parameters for multi-level TADAS dampers

Model	Elastic stiffness [kN/mm]	Ductility	Dissipated energy [kN.mm]
D-TADAS-5PL	11.38	11.51	7063.52
D-TADAS-3PL	3.82	8.38	3454.59
FD-TADAS-5PL	4.69	11.10	4956.09
SP-TADAS-2PL	109.16	34.55	19,200.68
TADAS-DIFFMAT	12.03	11.29	7036.06

ductility, and dissipated energy. To calculate these parameters, the obtained envelope curves in the previous sections for each model were linearized only in two forms of bi-linear or tri-linear diagrams using the recommended energy procedure by FEMA-356 (2000a) (Fig. 17). It is noteworthy that the elastic stiffness and dissipated energy were estimated as the slope of the first line and the area under the linearized curve, respectively. Moreover, the ductility was calculated as the ratio of the ultimate displacement and the effective yield displacement. Table 4 shows the calculated values of the mentioned parameters for multi-level TADAS dampers.

Regarding Table 4, it is seen that the SP-TADAS-2PL has the highest values for the considered parameters and the D-TADAS-5PL is in second place. But some important points should be considered to choose the best damper in this section, which are (1) excessive increase in stiffness can have negative effects such as increasing the spectral acceleration and consequently increasing seismic force and energy, (2) the buckling of the shear panel causes the pinching and instability of the obtained hysteretic curve and (3) in general, the average fracture strain of steel is 0.25 and according to Fig. 18, it can be seen that the SP- TADAS-2PL damper had a plastic strain of 0.73 and hence the corners of the shear

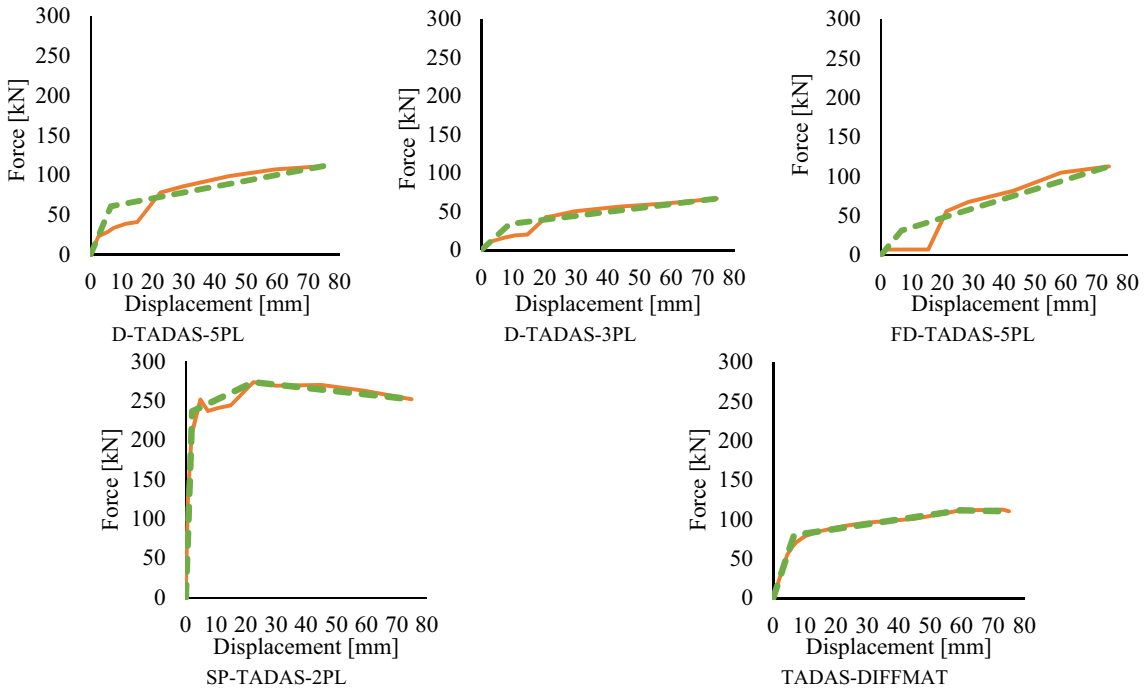

Fig. 17 The envelope (orange solid line) and linearized (green dashed line) curves of the considered multi-level TADAS dampers

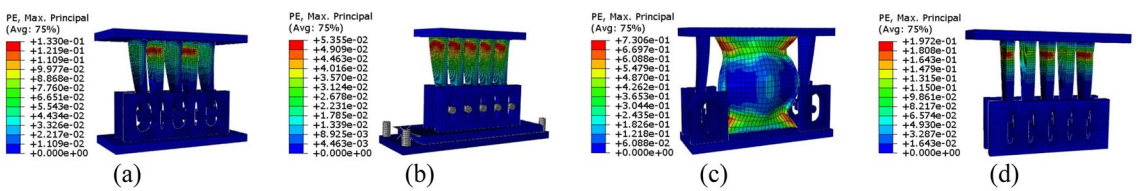

Fig. 18 The distribution of plastic strain in the considered multi-level damper models: **a** D-TADAS-5PL, **b** FD-TADAS-5PL, **c** SP- TADAS-2PL, **d** TADAS-DIFFMAT

panel were ruptured. In other words, the high amount of ductility and elastic stiffness in the SP-TADAS-2PL model is due to the highly ductile behavior of the steel shear panel. The high initial stiffness is one of the main desirable characteristics of steel shear panels and regarding the experimental results obtained in the research performed by Akbari Hamed and Mofid (2015a), it was seen that the values of demand partial ductility were high for the unstiffened steel shear panel. As the plastic mechanism of the unstiffened steel shear panel and the shear panel part of the SP-TADAS-2PL model is the post-buckling strength by the development of the tension-field action, therefore, the higher values of ductility for this type of multi-level TADAS damper seems normal. But, the important point to consider is that the average fracture strain of steel St37 is 0.25 and according to the obtained results from the numerical analysis of the SP-TADAS-2PL model, it is seen that this damper experiences the plastic strain value of 0.73 which demonstrates that the corners of the shear panel should be ruptured. Because, based on the observations from the experimental research carried out by Akbari Hamed and Mofid (2015a), the corners of the tested unstiffened steel shear panel were torn which confirms the aforementioned discussions. Therefore, based on the performed studies on the considered models of this research and according to the aforementioned points, among the two dampers D-TADAS-5PL and SP-TADAS-2PL, the D-TADAS-5PL model is introduced as the best multi-level TADAS damper.

The seismic performance of a building equipped with a multi-level TADAS damper

The building model

In this section, a 10-story two-dimensional moment-resisting frame (MRF) in a high-risk seismic zone was designed using the LRFD procedure by SAP2000 software. The story height was 3.2 m and the model had 5 spans with a length of 6.1 m. Also, the amount of distributed dead and live loads on the floors was considered as 500 kg/m^2 and 200 kg/m^2, respectively. Moreover, the assigned steel properties were the elastic modulus of 2.1×10^6 kg/cm^2 and yield strength of 2400 kg/cm^2 and the ultimate strength of 3500 kg/cm^2. Table 5 shows the list of the assigned profiles to the members of the designed model in which I-shaped and box cross sections were considered for the beams and columns, respectively.

As the seismic performance of this building model will be investigated using the IDA procedure, it was necessary to assign plastic hinges to the structural members of the designed frame. For this purpose, the bending plastic hinge of M3 along with the interactional plastic hinge of P-M3 was assigned to both ends of beams and columns, respectively, at relative distances of 0.05 and 0.95. Moreover, to perform a comparative study on the building equipped with a multi-level TADAS damper, the same designed MRF was considered in which the damper was located on top of the chevron braces. In the latter model, axial plastic hinges of P were assigned to the mid-point of the braces. It should be mentioned that the beam and column cross sections were chosen in such a way that the assigned profiles can satisfy the design specifications (e.g. AISC360, AISC341, ASCE7) for the greater values of force and moment demands calculated in both building models. Therefore, the assigned member profiles were kept constant in both building models to investigate only the effect of adding the multi-level TADAS dampers which were mounted on inverted-V chevron braces. It is noteworthy that properties of the assigned auto plastic hinges were calculated based on Tables 9–7.1 (Steel beams and columns-flexure) and 9–8 (Steel braces- axial) of the ASCE41-17. Given that the D-TADAS-5PL damper was selected as the best damper in Sect. 5, its envelope curve (Fig. 8b) was assigned to the force–deformation definition of the multi-linear plastic link element properties in the U2 direction with a Kinematic hysteresis type in SAP2000. To validate the accuracy of using the considered multi-linear plastic element for modeling the selected D-TADAS-5PL

Table 5 The assigned cross sections to the beams and columns

Story	Exterior beams	Interior beams	Exterior columns	Interior columns
1	IPE600	IPE600	Box380×254	Box400×254
2	IPE600	IPE600	Box380×254	Box380×254
3	IPE600	IPE600	Box300×191	Box380×254
4	IPE600	IPE600	Box300×191	Box380×254
5	IPE600	IPE600	Box300×191	Box380×254
6	IPE600	IPE600	Box300×191	Box320×191
7	IPE500	IPE550	Box250×191	Box300×191
8	IPE500	IPE500	Box250×191	Box300×191
9	IPE500	IPE450	Box250×191	Box250×191
10	IPE450	IPE450	Box250×191	Box200×127

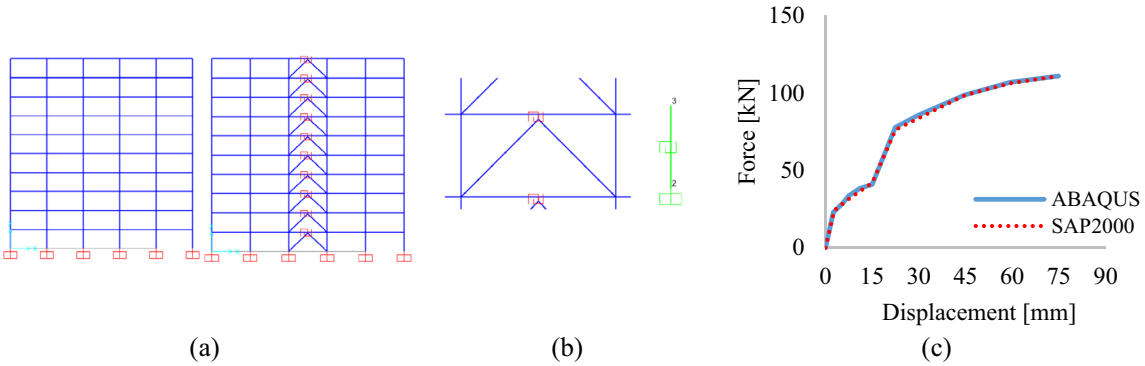

Fig. 19 **a** The considered building models with and without dampers, **b** A close-up view of the location of the damper and the single model of the D-TADAS-5PL damper, **c** comparison of the obtained monotonic force–displacement curves for a multi-linear plastic link and the D-TADAS-5PL model

damper, its single model (Fig. 19b) was pushed up to a lateral displacement of 75 mm using the nonlinear static analysis. As depicted in Fig. 19c, it is concluded that there is a good match between the pushover and envelope curves (Fig. 8b) which were obtained from SAP2000 and ABAQUS, respectively. It is noteworthy that the braces should remain in the range of elastic behavior, but in the finite element models the possibility of nonlinear behavior occurrence should be provided for different members of the building model; therefore, in addition to the definition of the multi-linear plastic link element properties, M3 and P-M3 plastic hinges, the axial plastic hinges were assigned to the braces. Figure 19 shows the considered building models with and without dampers along with a close-up view of the location of the damper.

The incremental dynamic analysis

The IDA is an analysis procedure that provides the magnitude of structural damage for different values of earthquake intensities using scaled accelerograms. It is noteworthy that these analyses are performed with the selection of a proper intensity measure (IM), which covers the full range of structural elastic to inelastic behavior up to the ultimate collapse status. Some parameters such as the peak ground acceleration (PGA), the peak ground velocity (PGV) and the spectral acceleration corresponding to the fundamental period of the structure with 5% damping (i.e. $S_a(T_1,5\%)$) can be considered as an appropriate IM. For assessment of the structural responses to seismic loads, some parameters such as the base shear, the connection rotation, the maximum ductility of stories, the maximum roof displacement, the maximum interstory drift ratio or various damage indices such as total cumulative dissipated energy, Park–Young index or the stability index proposed by Mehanny (2000), can be considered as the damage measure parameter (DM). In this study, to perform a comparative study on the buildings with and without dampers, the maximum interstory drift ratio (θ_{max}) and $S_a(T_1,5\%)$ were selected as the DM and IM, respectively, and they were analyzed under 11 seismic records (Table 6) to obtain the IDA curves. It should

Table 6 The characteristics of considered seismic records

Record	Station	PGA [g]	Duration [sec]	*R* [km]
Site–source distance > 10 km				
Imperial Valley	Calexico Fire	0.277	37.84	10.45
Kern County	Taft Lincoln School	0.159	52.9	38.89
Loma Prieta	Cliff House	0.076	40	78.5
Manjil	Abbar	0.515	53.5	12.55
Tabas	Dayhook	0.324	20.98	13
Site-source distance < 10 km				
Bam	Bam	0.808	49.6	1.7
Cape Mendocino	Petrolia	0.591	35.98	8.18
Erzincan	Erzincan	0.496	20.78	4.38
Loma Prieta	LGPC	0.57	25	3.88
Northridge	Rinaldi Receiving Sta	0.874	19.9	6.5
Tabas	Tabas	0.854	32.98	2.05

be noted that scaling the earthquake records based on the $S_a(T_1,5\%)$ considers the dynamic characteristics of the structure as well as the excitation characteristics. The earthquake records were selected based on the site-source distance so that some of them had a distance of less than 10 km and others had a distance of more than 10 km. Also, according to the record sets of FEMA-P695 (2009), the considered Cape Mendocino, Erzincan and Northridge records are in the pulse near-field records subset with the forward directivity effect, and the considered Manjil record is in the far-field record set. Figure 20 shows the pseudo-spectral acceleration spectrum for the selected records.

To have the same values for the $S_a(T_1,5\%)$ parameter of all records in IDA analyses and drawing the corresponding curves, the value of the $S_a(T_1,5\%)$ parameter of the records was first changed to 1 g by applying the $S_a(T_1)^1$ factor (Eq. 8) (Vamvatsikos & Cornell, 2005).

$$S_a(T_1)^1 = \frac{1}{S_a(T_1, 5\%)}. \tag{8}$$

Then, the scale factors of $S_a(T_1)^n$ were set using Eq. 9, starting from 0.1 g and increased to the extent that the horizontal part of the IDA curve was formed. The maximum value of the scale factor, which is shown by n_{max}, was estimated by the trial-and-error method for each record and it was dependent on the earthquake intensity in which the building model collapsed. In general, the considered interval for the scale factors was between 0.1 g and 0.2 g; but, in the range of inelastic behavior of the building model, smaller values were also considered.

$$S_a\left(T_1\right)^n = S_a\left(T_1\right)^1 \times n: \quad 0.1 \le n \le n_{\max}. \tag{9}$$

Global nonlinear dynamic instability is recognized by an arbitrarily large increase in displacement response subjected to a small increment in the IM (Jalayer & Cornell, 2009) and the flattening of the curve or encountering by the numerical non-convergence is an indicator of it (Vamvatsikos & Cornell, 2002a, 2002b). Moreover, the θ_{max} is known to relate well to global nonlinear dynamic instability (Vamvatsikos & Cornell, 2002a, 2002b) and the onset of global nonlinear dynamic instability occurs in θ_{max} values of more than 5% (Jalayer & Cornell, 2009). Regarding these explanations, in this study, the collapse criteria in the obtained IDA curves of the building models were selected as one of the points where the tangential stiffness was less than 20% of the elastic stiffness or the interstory drift ratio (θ_{max}) was equal to 10%, whichever occurred first (FEMA-350, 2000b; Vamvatsikos & Cornell, 2002a). Moreover, given a 5% damping ratio and considering the P-Δ effects, the nonlinear time history analyses were performed following the applied gravity load combination (i.e. 1.2 × dead load + live load) as the initial condition.

Results of IDA analyses

As depicted in Fig. 21, it was observed that after the softening point (i.e. the effective yield point) of the bare MRF, the structure became almost unstable dynamically and the DM increased sharply and moved toward collapse status with an approximately zero tangential stiffness. Whereas, in the models equipped with a damper, the effect of multi-level performance of the damper was observed. Moreover, an increase in the effective yielding point of these models was seen and the slope of the IDA curve did not become zero after the effective yielding point. It should be mentioned that the IDA curves of the MRF equipped with a damper show the DM return phenomenon (i.e. the weaving behavior) in most records which means that as the intensity of the earthquake increases, the structure sometimes experiences an increase in the DM and sometimes a decrease of it, and this can be a positive factor in increasing the strength of the structure and preventing its damage. Also, regarding the multi-level performance of the considered TADAS damper, it caused to observe the weaving behavior in the obtained IDA curves and due to the work starting of the main fuse of

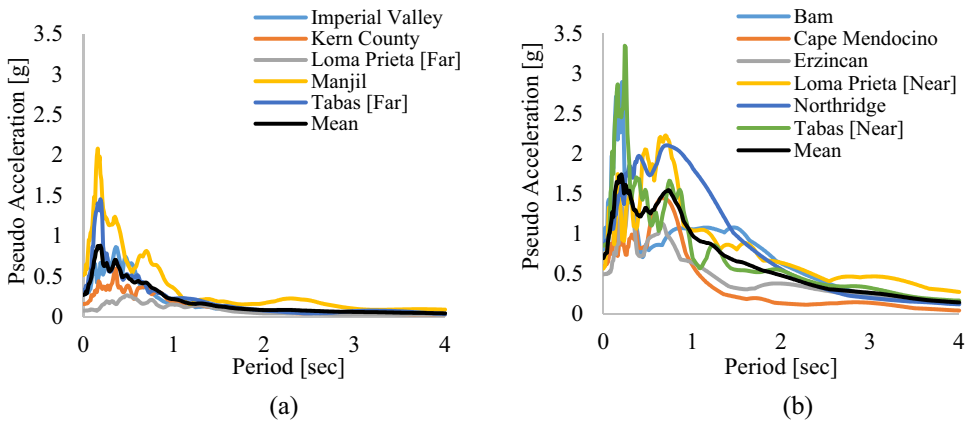

Fig. 20 The pseudo-acceleration spectrum of: **a** the records with $R > 10$, **b** the records with $R < 10$

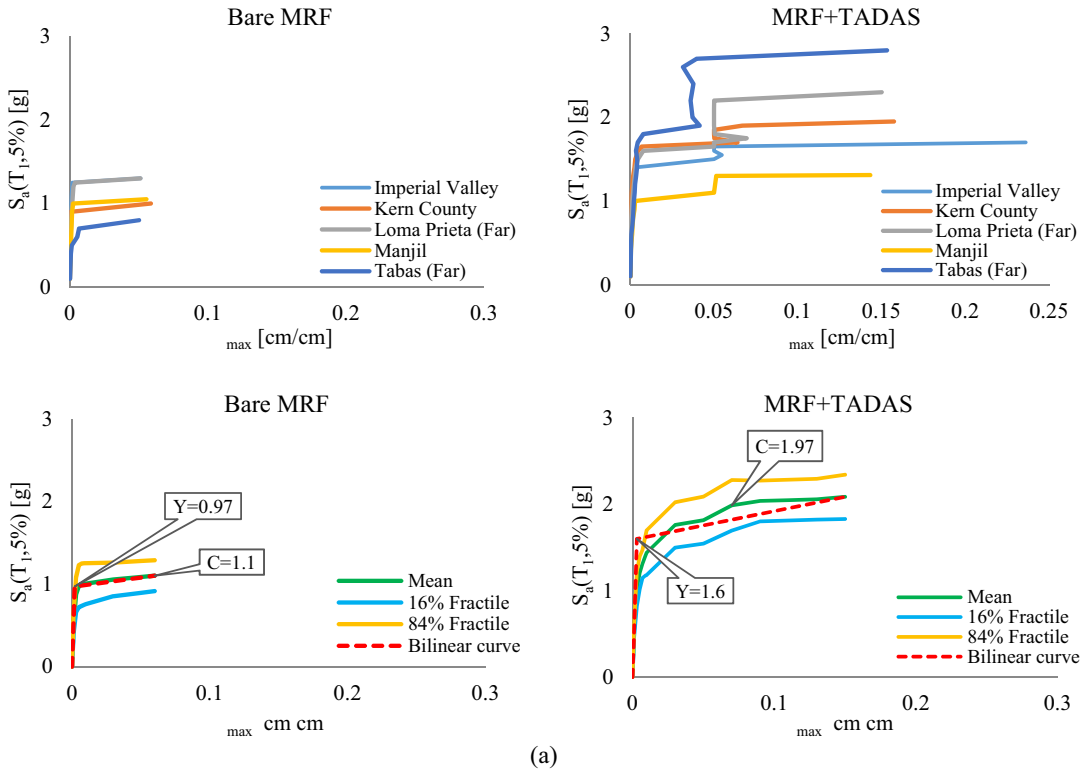

(a)

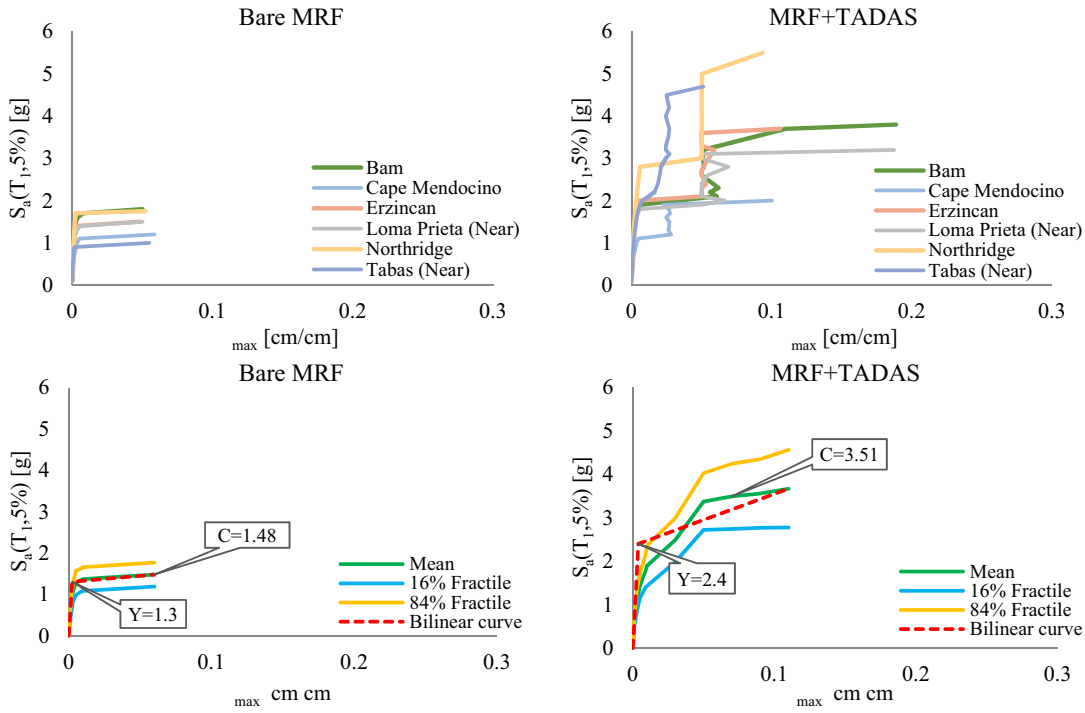

(b)

Fig. 21 The obtained IDA curves along with the corresponding mean, 16% and 84% fractile curves for the bare MRF and the MRF equipped with a multi-level TADAS damper under: **a** the records with $R > 10$, **b** the records with $R < 10$

the multi-level dampers, there was a recovery-like point in the IDA curves of the model with damper, which is seen in a θ_{max} of about 0.05 for the majority of considered records. In the obtained IDA curves, the corresponding θ_{max} value for the recovery-like point differs slightly and it can be concluded that this happens because of the time lag in the performance of the main fuse of the TADAS damper in different stories. It is noteworthy that due to changes in the amount of stiffness and damping of the system and hence the amount of base shear as a result of the installation of TADAS dampers, the plastic hinge development status was different in the considered building models and the braces remained elastic in all the performed IDA analyses. It can be mentioned regarding the obtained numerical results in this study which investigated the performance of only 2 building models subjected to incrementally intensified 11 earthquake records, the jumps were observed obviously in the obtained IDA curves; but it is required to study more building models with different characteristics to evaluate the occurrence of this jumping and the seismic performance of the considered multi-level TADAS dampers.

Tables 7 and 8 represent the obtained values for the effective yielding point and the collapse point of the MRF with and without damper under the considered seismic records. Regarding Fig. 21, the collapse criterion of a tangential stiffness of less than 20% of the elastic stiffness occurred earlier than the collapse criterion of a $\theta_{max} = 10\%$. It is observed that the considered collapse criteria in this research, as depicted in Fig. 21, cover the aforementioned definitions of global nonlinear dynamic instability. It is noteworthy that the obtained IDA curves were shown in Fig. 21 in two cases of the individual IDA curves for each record and their corresponding mean, 16% and 84% fractile curves. Moreover, the effective yielding point (i.e. Y) and the collapse point (i.e. C) were shown on the mean curve in which the Y was obtained by the bilinearized curve and the C point was determined in a point where the tangential stiffness was less than 20% of the elastic stiffness on the mean curve. According to

Table 7 Comparison of the corresponding IM values for the effective yielding point of the considered models

Record set	Record name	MRF + TADAS $S_a(T_1,5\%)$ [g]	Bare MRF $S_a(T_1,5\%)$ [g]	Difference [%]
R > 10 km	Imperial Valley	1.4	1.3	8
	Kern County	1.7	0.9	89
	Loma Prieta (Far)	1.6	1.3	23
	Manjil	1	1	0
	Tabas (Far)	1.8	0.7	157
R < 10 km	Bam	1.9	1.7	12
	Cape Mendocino	1.1	1.1	0
	Erzincan	2	1.4	43
	Loma Prieta (Near)	1.8	1.4	29
	Northridge	2.8	1.8	56
	Tabas (Near)	2	0.9	122

Table 8 Comparison of the corresponding IM values for the collapse point of the considered models

Record set	Record name	MRF + TADAS $S_a(T_1,5\%)$ [g]	Bare MRF $S_a(T_1,5\%)$ [g]	Difference [%]
R > 10 km	Imperial Valley	1.7	1.3	31
	Kern County	1.9	0.9	111
	Loma Prieta (Far)	2.2	1.3	69
	Manjil	1.3	1	30
	Tabas (Far)	2.7	0.7	286
R < 10 km	Bam	3.7	1.8	106
	Cape Mendocino	1.9	1.1	73
	Erzincan	3.6	1.4	157
	Loma Prieta (Near)	3.1	1.4	121
	Northridge	5	1.7	194
	Tabas (Near)	4.5	0.9	400

Tables 7 and 8, the multi-level TADAS damper had a significant effect on the enhancement of the seismic performance of the models along with the corresponding IM values at the effective yielding point and the collapse point of the building models. Regarding the individual IDA curves, it is concluded that for both record sets, the corresponding IM values for the effective yielding and collapse points of the MRF equipped with a multi-level TADAS damper were increased by 53.1% and 143.5% on average, respectively. Moreover, considering the achieved mean IDA curves, values of the aforementioned enhancements (i.e. Y and C) were on average 74.78% and 120.13%, respectively. It is noteworthy that the only difference between the considered new TADAS dampers in this study with the existing common type of TADAS damper (Mahmoudi & Abdi, 2012; Saeedi et al., 2016; Tsai et al., 1993) is the multi-level performance of them and there are no quantitative differences and performance enhancement in terms of the structural characteristics such as strength, stiffness, ductility and dissipated seismic energy. Regarding the obtained results of this study as depicted in Figs. 8, 10, 13, 15 and 21, it is concluded that the expected desired multi-level performance of these new TADAS dampers is achieved. If the intended arrangements for the multi-level performance of these TADAS dampers are removed, they will have exactly the same structural performance as the existing common TADAS dampers with the same geometrical and material properties and hence, their multi-level action will be eliminated.

As the fundamental period value of the considered residential building model equipped with the TADAS damper was 1.54 s, based on the Iranian Standard No. 2800, the approximate value of the pseudo-spectral acceleration of the design earthquake for a region of high seismicity on a site class of stiff soil equals to 0.515 g (i.e. given $R=1$ for the nonlinear dynamic analysis). Considering this fact that the pseudo-spectral acceleration values of the MCE earthquake achieve approximately by multiplying the corresponding values of the design earthquake by a coefficient of 1.5, it can be seen that the pseudo-spectral acceleration value for the MCE earthquake will be equal to 0.773 g, while the considered building models experienced much bigger values of pseudo-spectral acceleration in the performed IDA analyses of this study. Therefore, the seismic performance of the MRF equipped with the D-TADAS-5PL damper was evaluated implicitly for the maximum considered earthquake (MCE) level and the achieved results could be generalized to this earthquake level which is important for the evaluation of this system.

Conclusions

This study introduced the multi-level shear-bending TADAS damper and examined three types of multi-level TADAS dampers including (1) a TADAS made by different steel grade materials, (2) a TADAS combined with friction pads and (3) a TADAS with different pin hole sizes. To this aim, the considered finite element modeling procedure was validated based on the existing results of two experimental specimens. Then, five multi-level damper models with different energy dissipation mechanisms were examined using ABAQUS software under cyclic loadings. Finally, the best damper in terms of stiffness, energy dissipation, and ductility was selected. Then, a two-dimensional 10-story steel frame equipped with the selected multi-level damper was analyzed by the IDA method to investigate its seismic performance. The main results of this research are as follows:

1. Although the introduced SP-TADAS-2PL damper had the highest values for the considered parameters such as the elastic stiffness, ductility and dissipated energy; but, regarding the negative effects of the excessive increase in stiffness and the pinching of the hysteretic curve due to the buckling of the shear panel along with tearing of the shear panel with a plastic strain value of 0.73, the D-TADAS-5PL model introduced as the best multi-level TADAS damper. For a detailed study of the performance of the new SP-TADAS-2PL model, its experimental specimens should be tested under cyclic loads and the steel material failure (e.g. fracture) should be considered in the finite element modeling in future studies.
2. The D-TADAS-5PL damper had a stable hysteretic curve and its multi-level performance is easily adjustable on different earthquake hazard levels.
3. After the effective yield point of the bare MRF, the structure became almost unstable dynamically and the DM increased sharply and moved toward collapse status with approximately zero tangential stiffness.
4. According to the obtained results, multi-level TADAS dampers enhanced the seismic performance of the considered 10-story building model, significantly. It was concluded that for both record sets, the corresponding IM values for the effective yielding and collapse points of the MRF equipped with a multi-level TADAS damper were increased on average by 53.1% and 143.5%, respectively. Moreover, considering the achieved mean IDA curves, values of the aforementioned enhancements (i.e. Y and C) were on average 74.78% and 120.13%, respectively. It should be noted that only one 10-story building model was considered in this study and to generalize the obtained conclusions, it is required to perform IDA

analyses on more building models with different characteristics.

Author contributions The authors declare that no funds, grants, or other support were received during the preparation of this manuscript. The authors have no relevant financial or non-financial interests to disclose. All authors contributed to the study's conception and design. Material preparation, data collection and analysis were performed by Arash Akbari Hamed and Seyedeh Fatemeh Mortazavi. The first draft of the manuscript was written by Arash Akbari Hamed, Seyedeh Fatemeh Mortazavi and Mahsa Saeidzadeh and all authors commented on previous versions of the manuscript. All authors read and approved the final manuscript.

Funding The authors have not disclosed any funding.

Declarations

Conflict of interest The authors declare that no funds, grants, or other support was received during the preparation of this manuscript. The authors have no relevant financial or non-financial interests to disclose. All authors contributed to the study's conception and design. Material preparation, data collection and analysis were performed by Arash Akbari Hamed and Seyedeh Fatemeh Mortazavi. The first draft of the manuscript was written by Arash Akbari Hamed, Seyedeh Fatemeh Mortazavi and Mahsa Saeidzadeh and all authors commented on previous versions of the manuscript. All authors read and approved the final manuscript.

References

Abdollahzadeh, G. R., & Bayat, M. (2010). *The influences of the different PGAs and heights of structures on steel braced frame systems equipped with ADAS dampers*. Babol University of technology.

Akbari Hamed, A., & Mofid, M. (2015a). On the experimental and numerical study of braced steel shear panels. *The Structural Design of Tall and Special Buildings, 24*(14), 853–872.

Akbari Hamed, A., & Mofid, M. (2015b). On the plastic analysis of concentrically braced frames with shear panel, obtaining predetermined collapse mechanism. *The Structural Design of Tall and Special Buildings, 24*(5), 366–395.

Akbari Hamed, A., & Mofid, M. (2017). Plastic design of eccentrically braced frames with shear panels. *Proceedings of the Institution of Civil Engineers-Structures and Buildings, 170*(1), 17–32.

Alehashem, S.M.S., Keyhani, A. and Pourmohammad, H., 2008, October. Behavior and performance of structures equipped with ADAS & TADAS dampers (a comparison with conventional structures). In Proceedings of the 14th World Conference on Earthquake Engineering (pp. 12–17).

Dareini, H. S., & Hashemi, B. H. (2011). Use of dual systems in Tadas dampers to improve seismic behavior of buildings in different levels. *Procedia Engineering, 14*, 2788–2795.

Garevski, M. and Ansal, A. eds., 2010. Earthquake engineering in Europe (Vol. 17). Springer Science & Business Media.

Fahimi Farzam, M., & Kaveh, A. (2020). Optimum design of tuned mass dampers using colliding bodies optimization in frequency domain. *Iranian Journal of Science and Technology, Transactions of Civil Engineering, 44*(3), 787–802.

FEMA, 2000b. Recommended seismic design criteria for new steel moment-frame buildings. Report No. FEMA-350, SAC Joint Venture, Federal Emergency Management Agency, Washington, DC.

FEMA, 2000a. Prestandard and commentary for the seismic rehabilitation of buildings. Report No. FEMA-356, Federal Emergency Management Agency, Washington, DC.

FEMA, 2009. Quantification of building seismic performance factors. Report No. FEMA-P695, Federal Emergency Management Agency, Washington, DC.

Hamed, A.A. and Basim, M.C., 2020, December. Experimental-numerical study on weakened HSS-to-HSS connections using HBS and RBS approaches. In Structures (Vol. 28, pp. 1449–1465). Elsevier.

Hamed, A. A., Asl, R. B., & Rahimzadeh, H. (2021). Experimental and numerical study on the structural performance of auxetic-shaped, ring-shaped and unstiffened steel plate shear walls. *Journal of Building Engineering, 34*, 101939.

Hosseini Hashemi, B., & Moaddab, E. (2017). Experimental study of a hybrid structural damper for multi-seismic levels. *Proceedings of the Institution of Civil Engineers-Structures and Buildings, 170*(10), 722–734.

Jalayer, F., & Cornell, C. A. (2009). Alternative non-linear demand estimation methods for probability-based seismic assessments. *Earthquake Engineering & Structural Dynamics, 38*(8), 951–972.

Kaveh, A., Fahimi Farzam, M., & Hojat Jalali, H. (2020b). Statistical seismic performance assessment of tuned mass damper inerter. *Structural Control and Health Monitoring, 27*(10), e2602.

Kaveh, A., Fahimi Farzam, M., Hojat Jalali, H., & Maroofiazar, R. (2020a). Robust optimum design of a tuned mass damper inerter. *Acta Mechanica, 231*(9), 3871–3896.

Kaveh, A., Pirgholizadeh, S., & Khadem, H. O. (2015). Semi-active tuned mass damper performance with optimized fuzzy controller using CSS algorithm. *Asian Journal of Civil Engineering, 16*(5), 587–606.

Kelly, J. M., Skinner, R. I., & Heine, A. J. (1972). Mechanisms of energy absorption in special devices for use in earthquake resistant structures. *Bulletin of the New Zealand Society for Earthquake Engineering, 5*(3), 63–88.

Li, H., Li, G. and WANG, S., 2014, July. Study and Application of Metallic Yielding Energy Dissipation Devices in Buildings. In Proceedings of the 10th US National Conference on Earthquake Engineering. Anais de conferência.

Li, Z., Shu, G., & Huang, Z. (2019). Development and cyclic testing of an innovative shear-bending combined metallic damper. *Journal of Constructional Steel Research, 158*, 28–40.

Mahmoudi, M., & Abdi, M. G. (2012). Evaluating response modification factors of TADAS frames. *Journal of Constructional Steel Research, 71*, 162–170.

Mehanny, S.S.F., 2000. Modeling and assessment of seismic performance of composite frames with reinforced concrete columns and steel beams. Stanford University.

Mosayebi, M., Sahab, M.Q., Saeedi, S., 2016. Modification of the performance of TADAS dampers under different earthquake levels. In Proceedings of the 1st International Conference on Urban, Civil and Architectural Engineering, Ghom, Iran.

Nobari, H.B. and Hamed, A.A., 2017. 03.25: On the seismic behavior of the HBS and RBS moment connections. ce/papers, 1(2–3), pp.702–710.

Payne, T., 2000. Nonlinear response of steel beams. US Department of the Interior, Bureau of Reclamation, Dam Safety Office.

Rezaei, S., Hamed, A. A., & Basim, M. C. (2020). Seismic performance evaluation of steel structures equipped with dissipative columns. *Journal of Building Engineering, 29*, 101227.

Ribakov, Y., Gluck, J., & Reinhorn, A. M. (2001). Active viscous damping system for control of MDOF structures. *Earthquake Engineering & Structural Dynamics, 30*(2), 195–212.

Saeedi, F., Shabakhty, N., & Mousavi, S. R. (2016). Seismic assessment of steel frames with triangular-plate added damping and stiffness devices. *Journal of Constructional Steel Research, 125*, 15–25.

Saeidzadeh, M., Chenaghlou, M.R. and Akbari Hamed, A., 2022b. Evaluation of the structural behavior of a novel self-centering beam-column connection with friction damper in comparison to existing connections. Journal of Civil and Environmental Engineering.

Saeidzadeh, M., Chenaghlou, M. R., & Hamed, A. A. (2022a). Experimental and numerical study on the performance of a novel self-centering beam-column connection equipped with friction dampers. *Journal of Building Engineering, 52*, 104338.

Skinner, R. I., Kelly, J. M., & Heine, A. J. (1974). Hysteretic dampers for earthquake-resistant structures. *Earthquake Engineering & Structural Dynamics, 3*(3), 287–296.

Standard-2800 (4th edition), 2014. Iranian seismic provisions standard. Road, Housing and Urban Development Research Center, Tehran.

Tsai, K. C., Chen, H. W., Hong, C. P., & Su, Y. F. (1993). Design of steel triangular plate energy absorbers for seismic-resistant construction. *Earthquake Spectra, 9*(3), 505–528.

Vamvatsikos, D. and Cornell, C.A., 2002a, February. The incremental dynamic analysis and its application to performance-based earthquake engineering. In 12th European Conference on Earthquake Engineering (Vol. 479).

Vamvatsikos, D., & Cornell, C. A. (2002b). Incremental dynamic analysis. *Earthquake Engineering & Structural Dynamics, 31*(3), 491–514.

Vamvatsikos, D., & Cornell, C. A. (2005). *Seismic performance, capacity and reliability of structures as seen through incremental dynamic analysis* (p. 151). Stanford University, Report No.